Computational Materials Science 127 (2017) 204–210

Contents lists available at ScienceDirect

Computational Materials Science

journal homepage: www.elsevier.com/locate/commatsci

First-principles study of codoping TiO_2 systems capable of improving the specific surface area and the dissociation of H_2O to generate H_2 and O_2

Cecilia I.N. Morgade [a,b], Gabriela F. Cabeza [a,*]

[a] Grupo de Materiales y Sistemas Catalíticos, IFISUR, UNS, CONICET, Depto de Física, Av. Alem 1253, Bahía Blanca B8000CPB, Argentina
[b] Universidad Tecnológica Nacional, 11 de Abril 461, Bahía Blanca B8000LMI, Argentina

ARTICLE INFO

Article history:
Received 11 September 2016
Received in revised form 24 October 2016
Accepted 29 October 2016

Keywords:
TiO_2
Density functional theory
Codoping
Water splitting
Electronic structure

ABSTRACT

In this study, theoretical results of structural, electronic and magnetic properties of codoped anatase TiO_2 using metals (Pt, V) and nonmetals (C, N) to obtain insight into the codoping effect are reported. Results of monodoped systems with N, C, V and Pt are also reported. The way different pairs of metal-nonmetal dopants affect the positions of the edge of the valence and conduction bands, and consequently their redox potential in the search for the best candidate for water splitting into H_2 and O_2 has also been studied. In this sense, density functional calculations show that the particular case of Pt-C@Ti codoped TiO_2 would be the most efficient for the mentioned reaction. In addition, it is pointed out that the formation of particular structures observed is due to the interaction metal-nonmetal (M-NM) rather than the particular nature of the foreign atoms. The analysis also shows that the systems presenting the highest interplanar spacing in the crystal structure are V-C@O and Pt-C@O, unlike Pt-N@O that has not shown significant modifications. This could translate into an enhancement in the specific surface area, particularly observed in the case of V-C@O.

1. Introduction

Titanium dioxide (TiO_2) has characteristics which make it very interesting for the design of catalytic technologies applicable to devices. Various feasible modifications may be made to the material to give it great versatility adding it value as engineering materials. The theoretical and experimental studies of the modified oxide carried out to the present have given conflicting results, so further studies are needed to provide clarity. Possibly the controversy may be because there are many interacting factors involved in modifying oxide. In particular, the interactions of metallic and nonmetallic dopants are greatly influenced not only by the nature of the doping elements, but also by the position thereof in the crystal lattice.

In a work recently published by our group [1] it was reported that the codoped of titania in anatase structure with C-doping in O site and Pt-doping in Ti site leads to the formation of peculiar and symmetrical structures that brings about distortion in the mesh. Such distortion increases the distances between planes and could generate reactive surfaces at high dopant concentrations. This study attempts to resolve whether the above structures would either be formed by the particular nature of C and Pt elements as dopants or if they are due to the interaction metal-nonmetal as has been reported by other authors [2]. As it is known, carbon can have both anionic and cationic behavior and can form multiple bonds because of its different possible hybridizations (sp, sp^2 and sp^3), while platinum is a noble metal despite having large number of valence electrons.

Is the formation of these structures due to the nature of this pair metal (M) – nonmetal (NM), Pt and C, or each of the individual dopants? To answer this question, different possibilities of cationic and anionic substitution were studied: V instead of Pt because it provides magnetic properties, and N instead of C, which is an element with odd number of external electrons.

Motivation in seeking answers to the formation of these structures is that it is known that a higher specific area corresponds to better catalytic activity [3,4]. Considering that the specific surface area is the relationship between the surface and its mass, this can be increased if the solid is distorted or has fractures or pores inside. This is reflected in a higher real exposed surface that would be calculated assuming a geometric shape.

A second important objective of this work is to determine which of the cases studied is the best candidate for the photoelectrochemical water splitting reaction-of interest in hydrogen production [5,6] and environmental remediation [7,8].

* Corresponding author.
E-mail address: gcabeza@uns.edu.ar (G.F. Cabeza).

http://dx.doi.org/10.1016/j.commatsci.2016.10.038
0927-0256/

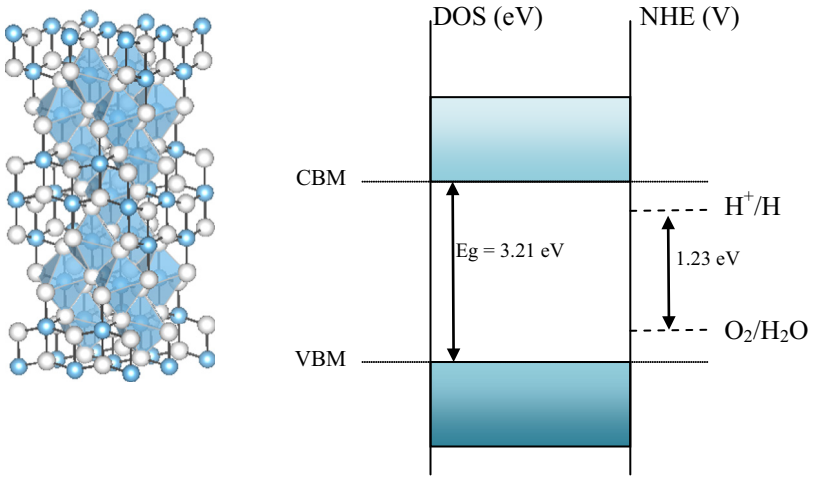

Fig. 1. Position of the band edges of TiO_2 anatase (left) relative to the standard potentials at pH = 0 as referenced to the normal hydrogen electrode (NHE). Eg represents the band gap width obtained for our group.

As schematized in Fig. 1, water splitting process [5,9] makes use of the reducing and oxidation potentials of TiO_2 and could be enhanced if the edges of their valence band (VB) and conduction band (CB) approach the appropriate redox potential. The reduction potential is measured by the conduction band minimum (CBM) energy while the oxidation potential is measured by the valence band maximum (VBM) energy. The design principle of the catalyst should consider that the closer the CBM energy to the vacuum level, the stronger the reducing potential is, whereas the lower the VBM energy, the higher the oxidizing potential is. For example, to make the spontaneous production of H_2 and O_2 from water dissociation possible, the band edges must include the water redox potential levels; i.e., the oxygen and hydrogen reactions must lie between the VBM and CBM [10–12].

The reduction and oxidation equations of H_2O are displayed below:

$$2H_2O + 2e^- \rightarrow H_2 + 2OH^- \quad (1)$$

$$O_2 + 4e^- + 4H^+ \rightarrow 2H_2O \quad (2)$$

The reduction potential of water has a value of −0.83 eV, while the oxidation potential value is −1.23 eV. Moreover, it is known that water undergoes a process of auto-ionization:

$$2H_2O \leftrightarrow H_3O^+ + OH^- \quad (3)$$

This reaction has a low equilibrium constant ($K = 10^{-14}$) that can be displaced by Le Chatelier's principle towards the generation of H_3O^+ whose reduction potential is 0.00 eV:

$$2H^+ + 2e^- \rightarrow H_2 \quad (4)$$

The hypothesis that arises is that codoping using donor-acceptor pairs, M-NM, could passivate the holes in the acceptor levels of impurities keeping the semiconductor character of the system. Moreover, an important relationship exists between the electrode potential, CBM (or Ec edge), VBM (or Ev edge) and Eg that can be approximately expressed by the equations:

$$Ec(V \text{ vs NHE}) = 1.23 - \frac{Eg(eV)}{2} \quad (5)$$

$$Ev(V \text{ vs NHE}) = 1.23 + \frac{Eg(eV)}{2} \quad (6)$$

with the exception of some transition metal oxides which have filled or partly filled *d* orbitals, as shown in reference [11]. From the electronic structures of systems with *n-p* impurities, as well as from these equations, it is possible to obtain a quantitative location of Ec and Ev which should meet the redox capacity.

Also, as it is known for titania, the electrons in the VB need radiation of about 380 nm or less so as to access the CB. The VB is located deep in energy generating holes with high oxidative potential; nevertheless, the electrons that reached the CB do not have an appropriate reducing potential, being this effect more pronounced in rutile (R) than in anatase (A). The doping of the system with different anions (C, N) at O sites [12,13], or cations (Cr, V, Fe, Ni, Pt) [14,15] induces changes in the positions of the band edges that in turn, involve shifts of their both oxidation and reduction potential.

Part of the aim of this work is also to provide theoretical results of structural, magnetic and electronic properties of codoped anatase TiO_2 using Pt, V as metals and C, N as non-metals, to obtain insight into the M-NM codoping effect. With the intention to complete the study, a section referring to results obtained for monodoping with nonmetals (C, N) and metals (Pt, V) has been incorporated.

2. Theoretical framework

Density Functional Theory calculations were carried out by using the Vienna Ab-Initio Simulation Package (VASP) code [16] and the projector augmented-wave method (PAW) developed by Blöch to describe the ion-electron interactions [17]. The generalized gradient approximation due to Perdew and Wang (GGA-PW91) [18] was adopted to treat exchange-correlation effects between valence electrons. The basis of plane waves were generated considering 4 valence electrons for Ti ($3d^34s^1$), 5 valence electrons for V ($3d^44s^1$),10 valence electrons for Pt ($5d^96s^1$), 4 valence electrons for C ($2s^22p^2$), 5 valence electrons for N ($2s^22p^3$) and 6 valence electrons for O ($2s^22p^4$). The smooth part of the wave functions was expanded in planes waves with a kinetic energy cutoff of 450 eV. The Brillouin zone integration was performed on well-converged Monkhorst-Pack k-point meshes [19]. For the k-point integration, we used $3 \times 3 \times 3$ mesh for the $(3 \times 3 \times 1)$ anatase supercell of 108 atoms in order to represent the anatase codoped system with low concentrations of impurities. The convergence criteria for the electronic and ionic relaxation were 0.1 meV and 20 meV/Å, respectively. The known drawback that the DFT strongly underestimates the band gap of complex oxide materials has been

discussed at length in the literature. A viable approach to resolve the self-interaction errors for strongly correlated electron materials is the use of methods known as DFT+U. The usual application of this method introduces a correction of the DFT energy by means of single numerical parameters, U-J (U and J are screened Coulomb and exchange parameters, respectively) involve different aspects of self-interaction. This method was originally proposed by Anisimov and co-workers [20] to account for correlations resulting from strong on-site Coulomb and exchange interactions. In this model a specific number of localized orbitals is selected and the associated electron correlation is treated, depending highly on the choice of the (Hubbard) parameter U used [21]. In this work, we use the Dudarev's approach [22] implemented in the VASP through careful selection of U, achieving excellent matches with the experimental band gap and bulk modulus measured for the systems investigated. The U value was optimized to a value of 8 eV [23] for corrections of Coulomb interactions of the Ti and V *d* electrons and it was previously proposed by our group with excellent results [1,24]. Moreover, the study involves the effect of the U on the lattice parameters, bulk modulus and thermal properties as heat capacity at constant volume (Cv) for the stoichiometric systems. All calculations were performed at the spin polarized level.

For each optimized structure the density of states (DOS) was calculated to obtain the corresponding electronic structure and band gap value (Eg). The study was completed evaluating the corresponding magnetic moments for the atoms (μ in μ_B) and Bader charge [25] analysis was done to analyze charge populations in the periodic calculations. The interatomic distances, angles and cell parameters and the isosurfaces were obtained using VESTA [26].

The formation energies (E_{for}) of codoped systems were calculated following the procedure according to the equations given in reference [1]; the most favorable structure has the lowest energy. Furthermore, in order to improve the knowledge of these systems and to explore if the codoping system is stable, it is possible to calculate the codoped pair binding energy (E_b) as discussed in reference [27]:

$$E_b = E_M + E_{NM} - E_{codoped} - E_{pure}$$

where E_M, E_{NM}, $E_{codoped}$ and E_{pure} are the total energy of metal (M) monodoping (Pt, V) in TiO_2, nonmetal (NM) monodoping (C, N) in TiO_2, codoping in TiO_2 and pure anatase TiO_2, respectively. The same supercell was used in all calculations. A positive value of E_b indicates that the donor-acceptor pairs are likely to bind each other when both of them are presented in the host.

3. Results and discussion

As it has been previously mentioned, with a view to complete the knowledge of the doped systems, a section with the results obtained for monodoping was included (Table 1). From the optimized structures, we proceeded to the analysis of Bader charges, magnetic moments (μ) and electronic structure. Simply for reasons of convenience, the zero energy was set at the VBM, including the values of the valence band, conduction band and Eg widths and the energy location of the defect states in the band-gap, always measured from CBM. Similar analysis was performed for the five codoped systems studied including the interatomic distances M-NM of interest in the calculation of specific surface area. The main results obtained are summarized in Table 2.

3.1. Monodoping

In order to represent the anatase doped with nonmetal, carbon and nitrogen atoms are placed in an oxygen site (C@O, N@O) as well as in interstitial site (Ci, Ni). In addition, only substitutional C is incorporated on Ti-site (C@Ti). The corresponding contribution in weight percent (wt%) at low concentrations are comparable to those used in some experimental studies and are indicated in Table 1.

Doping metals is modeled by replacing a Ti atom by Pt (Pt@Ti) or V (V@Ti) and at interstitial site in the case of V(Vi). The respective structures of some cases studied are shown in Fig. 2

In the case of anionic substitution in anatase titania, when an oxygen atom is replaced by one carbon or nitrogen atom, C@O and N@O, the system becomes one *p*-type dopant, as noted by their electronic configurations. These systems are more oxidizing than anatase pure since they add holes to the lattice being this effect more pronounced for C which shifts the valence band towards lower energies. At low impurities concentrations, the most stable site for the N is the anionic substitution.

On the other hand, when these nonmetals are incorporated into interstitial sites, they act by increasing the number of electrons in the crystal, as dopants *n*-type, with reducing character and the corresponding band gap widths are decreased. In the case of carbon at low concentrations, one structure type distorted tetrahedron is observed [1] which also turns to be the most stable site (Table 1). In these cases, C acquires cationic characteristics being its charge +4*e*, while when placed at oxygen site, it acquires negative charge (Table 1) and no particular structures are evident. On the other hand, when C is located in substitution of Ti atom, the charge acquired is also +4*e* and internal structures such as CO_2 could be observed. Such structures present C—O bond lengths located

Table 1
Information of the contribution in weight percent (wt%) and the main features of the cell parameters, electronic structure and Bader charges values of dopants (q) for monodoping. VB and CB are the widths of the valence and conduction bands. The position of the defect states in the band-gap are measured from CBM. For E_{for} see text. The value of the wavelength (λ) is given as a reference of absorption edge. Actually the requirement is to red-shift the absorption edge of TiO_2 to wavelengths longer than 400 nm.

	C@O	N@O	Ci	Ni	C@Ti	Pt@Ti	V@Ti	Vi
wt%	0.4	0.5	0.4	0.5	0.4	6.4	1.8	1.7
a (Å)	3.91	3.98	4.01	4.03	4.07	3.95	3.95	4.02
b (Å)	3.92	3.98	4.02	4.05	4.07	3.95	3.95	4.03
c (Å)	9.47	9.89	10.06	10.11	10.06	9.69	9.69	9.99
E_{for} (eV)	3.18	1.22	−6.13	0.68	4.43	1.83	3.32	−1.89
Eg (eV)	3.19	2.87	3.04	3.02	3.02	3.34	3.16	1.72
λ (nm)	389	432	408	411	411	371	392	720
VB (eV)	4.61	4.42	4.36	4.37	4.27	4.57	4.65	5.73
CB (eV)	1.86	1.65	1.93	1.66	1.67	1.76	1.84	6.68
States in the band-gap	3.01–2.92–0.80	2.85	2.53	None	None	0.44–2.64–2.81	None	0.69
q_{dop} (*e*)	−1.16	−1.27	4.00	−0.07	4.00	1.81	1.22	0.63

Table 2
Information of the main features of the electronic structure, Bader charges values of dopants (q), distance between metal (M) and nonmetal (NM) and magnetic moments (μ) values of dopant atoms. The position of the defect states in the band gap are measured from CBM. VB and CB are the widths of the valence and conduction bands. For ΔE_V, ΔE_C, E_{for} and E_b see text.

	Undoped	Pt-C@O	Pt-N@O	V-C@O	Pt-Ci	Pt-C@Ti
a (Å)	3.96	4.00	4.00	3.99	4.01	3.99
b (Å)	3.96	4.00	4.01	4.00	4.03	4.02
c (Å)	9.76	9.95	9.96	9.97	10.02	9.95
E_{for} (eV)	–	2.58	1.25	−3.52	−1.33	3.27
E_b (eV)	–	2.86	−0.22	10.08	−2.55	3.42
Eg (eV)	3.21	3.20	3.20	3.11	3.04	*3.03*[a]
VB (eV)	4.53	4.41	4.41	4.49	4.61	4.66
CB (eV)	2.06	1.64	1.64	1.64	1.78	1.73
ΔEg (eV)	–	−0.01	−0.01	−0.10	−0.17	*−0.18*
ΔE_V (eV)	–	−0.70	−0.61	−0.76	−0.87	*0.28*[a]
ΔE_C (eV)	–	−0.79	−0.71	−0.95	−1.12	*−0.02*[a]
States in the band-gap	–	0.4–2.7–3.0	0.5–2.7	1.1–2.9	0.5	0.6–0.3
qPt (*e*)	–	1.76	1.76	–	1.76	1.74
qV (*e*)	–	–	–	2.45	–	–
qC (*e*)	–	−1.09	–	−1.31	1.63	4.00
qN (*e*)	–	–	−1.29	–	–	–
dM-NM (Å)	–	6.09	6.05	6.02	3.01	4.86
μPt (μ_B)	–	–	–	–	0.01	–
μV (μ_B)	–	–	–	0.81	–	–
μC (μ_B)	–	–	–	0.28	–	–
μN (μ_B)	–	–	0.55	–	–	–

[a] Optimal values for the redox reaction of H_2O to produce H_2 and O_2 are highlighted in italics.

between the ones formed by a single covalent bond and a double one. Possibly, the formation of these internal structures is related to the high value of formation energy.

Otherwise, when nitrogen is interstitially located in anatase, a structure type NO^- (Fig. 2b) can be assumed where the dopant atom acquires a net negative charge (−0.07e).

The complicated implications involved in nonmetals as dopants explain the controversy of published experimental results [28,29]. The theoretical study demonstrated the complexity of the specific effects of the dopant nature (type *n* or *p*); the formation of individuals structures stabilized within the solid depends not only on the impurities position in the network, but also on the concentration and polymorph type [1].

In reference to the monodoping with metals, we can mention that the substitutional doping at low concentrations is less expensive in the case of Pt than V. The doped with interstitial V is always exergonic. It may be also remarked that all Pt doped systems are nonmagnetic, while if the substitutional dopant metal is V, the magnetic moment is 1 μ_B per cell, lower if we compare with the 5 μ_B per cell obtained for interstitial doped vanadium. This high value makes this metal an interesting candidate as the dopant for generation of spintronic materials time. The amount of electrons supplied to the crystal by the metal presence (*n*-type dopant) is greater especially when the metals are located at interstices (for example V) causing a greater band shift to lower energies. The corresponding DOS curves are displayed in Fig. 3

3.2. Codoping

The photocatalytic mechanism in titania has been discussed at length in the literature. More recent experimental studies showed that monodoping using cations or anions has not reached the expected efficiency in regard to improving the photocatalytic titania capacity. Various side-effects such as: systems becoming unstable, recombination of photo-excited electron-hole pairs, reducing the carried mobility, are unfavorable to enhance the photocatalytic efficiency. However, the donor-acceptor codoping concept can improve semiconducting material quality. To explore new combinations, different M-NM pairs are proposed. For example, the structures of co-doped V-C@O and Pt-N@O anatase are shown in Fig. 4.

Firstly, it is important to emphasize the great agreement of the calculated Eg of pure anatase TiO_2 (3.21 eV) with the experimental result of 3.2 eV. The more relevant characteristics of the Pt-C-codoped anatase presented in detail in reference [1] were included in Table 2 to facilitate the comparison. The energy difference between the valence bands (ΔE_V) and conduction bands (ΔE_C) with respect to pure anatase, also indicated in Table 2, are important parameters for analyzing the photoelectrochemical activity of the titania as mentioned in the introduction. The redox potentials of water have been drawn up on Fig. 5 in red[1] broken line to bring about clarity.

Let us present here the results corresponding to Pt-N@O and V-C@O. For the first one, similar characteristics to Pt-C@O are observed in the electronic structure when the nonmetal dopant is nitrogen. The Eg remains almost unchanged compared to undoped anatase and N-doping also creates localized states below the conduction band edge at 0.52 eV and 2.68 eV and up/down N 2*p* states lying further down from the valence band at 0.87 eV. However, it should be noted that this system is magnetic with a magnetic moment for the N atom of 0.55 μ_B obtained from the bulk calculations unlike Pt-C@O system. Another similitude to be mentioned, although not as pronounced, is that when the NM is N instead of C, the increase in the separation between the plane containing the NM dopant and the plane above it, evidenced by the distance between the NM and the O located just on top (Ot) of NM is also observed (Fig. 6 and Table 3).

When the metal dopant is vanadium (V-C@O), the system is magnetic with a magnetic moment for the V atom of 0.81 μ_B. The formation of isolated impurity energy levels below the CBM can be related to the charge transfer from the 3*d* orbital of V ions to the conduction band of TiO_2. Similar behavior has been reported recently [30,31]. These kinds of impurity energy levels could act

[1] For interpretation of color in Fig. 5, the reader is referred to the web version of this article.

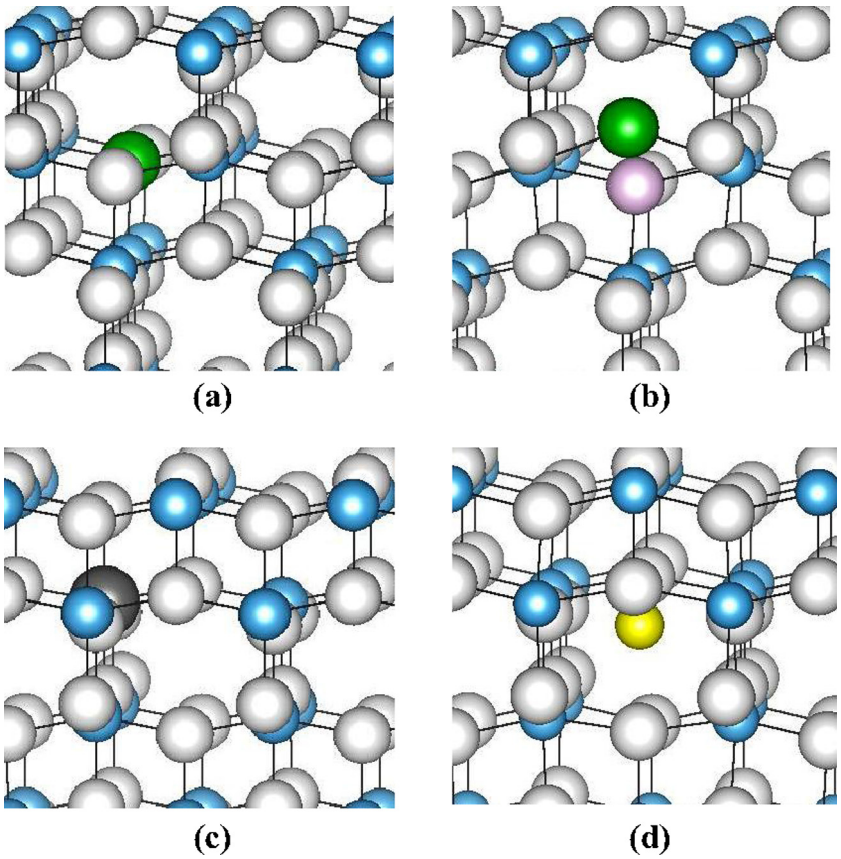

Fig. 2. Partial geometry of the monodoping models N@O (a), Ni (b), Pt@Ti (c) and Vi (d) anatase. The white spheres represent O atoms, the light blue spheres represent the Ti atoms, the green sphere represents the N impurity and the gray/yellow sphere represents the Pt/V atoms respectively. With light pink we represent the O atom in the NO^- complex (see text). (For interpretation of the references to color in this figure legend, the reader is referred to the web version of this article.)

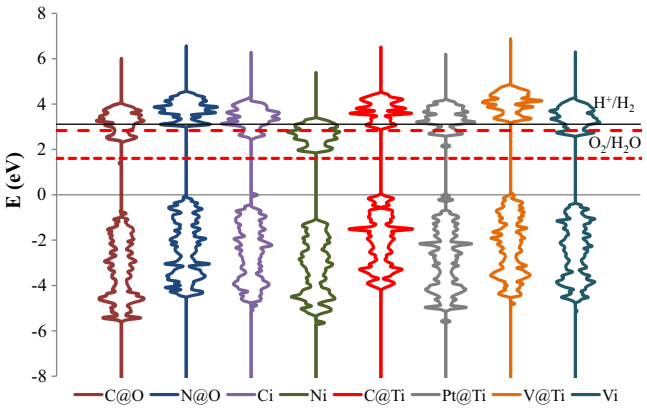

Fig. 3. Comparative density of states (DOS) of the different cases studied of monodoped anatase. The VBM of pure anatase is set to zero. A horizontal line is drawn on the conduction band bottom (CBM) of pure anatase as a guide for the eyes. The redox potentials of water have been drawn up on in red broken line. (For interpretation of the references to color in this figure legend, the reader is referred to the web version of this article.)

as acceptor levels, which can reduce the recombination rate of charge carriers and thus improve the photocatalytic activity of titania.

Regarding the obtained values for E_{for} and E_b, we can appreciate that this system has the most favorable structure (−3.52 eV) and is the most stable codoping system (10.08 eV) in comparison with the other structures analyzed. However, considering the location of their bands, this structure does not have the appropriate values for water splitting.

On the other hand, this system exhibits a considerable increase in the interplanar spacing, resulting from codoped (Δd value). This could translate into an enhancement in the surface area. We estimate an increment of the specific surface area of about 33.5 m^2/g for the position dopants, distances M-NM and concentration considered. Experimentally, this value depends strongly on the conditions of synthesis as shown in Ref. [32]; different V-TiO_2 series gave specific surface area over 110 m^2/g while others ranged from 37 to 47 m^2/g.

We now turn to the results corresponding to Pt-C-codoped in particular, Pt-C@Ti. We should note that a high E_{for} value was obtained for this system. On the other hand, the formation of an internal structures type CO_2 in the case of C@Ti monodoping is highlighted in Section 3.1, also observed by another group [1,33]. The most likely explanation is that the formation of this CO_2 structure could be responsible for the E_{for} value obtained for Pt-C@Ti. If we subtract to this energy, the necessary energy for the formation of CO_2 (4.06 eV according to reference [34]), it would be obtained a E_{for} value of −0.79 eV for Pt-C@Ti.

It is now useful to make a few remarks on the electronic structure. From the results of the analysis of the density of states summarized in Table 2 and shown in Fig. 5, we can infer that from the codoped studied systems, it is the one that presents the greatest reduction of the Eg with respect to pure anatase (−0.18 eV), the lower shift of the conduction band (−0.02 eV) and the most favorable adjustment of the position of valence band (0.28 eV). These observations are in agreement with a greater reduction in the energy required for electron excitation as well as the reduction potential. All mentioned conditions are desirables to the redox water splitting reaction because it would be the most efficient both to oxidize water to produce O_2 as to reduce it generating H_2.

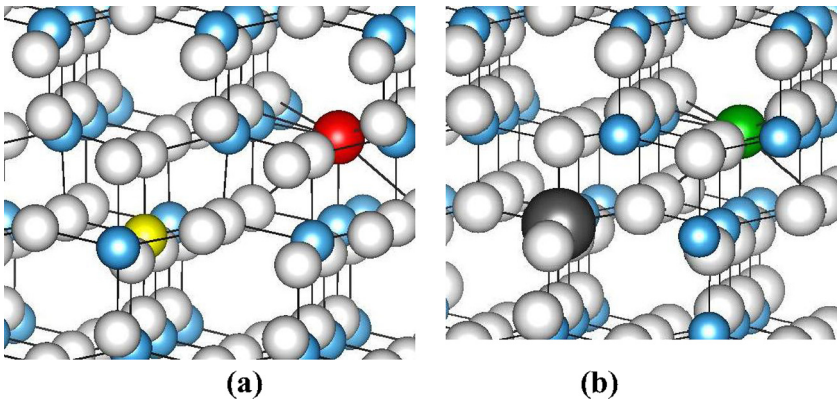

Fig. 4. Partial geometry of the models for V-C@O codoped (a) and Pt-N@O codoped anatase (b). The white spheres represent O atoms, the light blue spheres represent the Ti atoms, the gray/yellow sphere represents the Pt/V atom and the red/green sphere represents the C/N impurity respectively. (For interpretation of the references to color in this figure legend, the reader is referred to the web version of this article.)

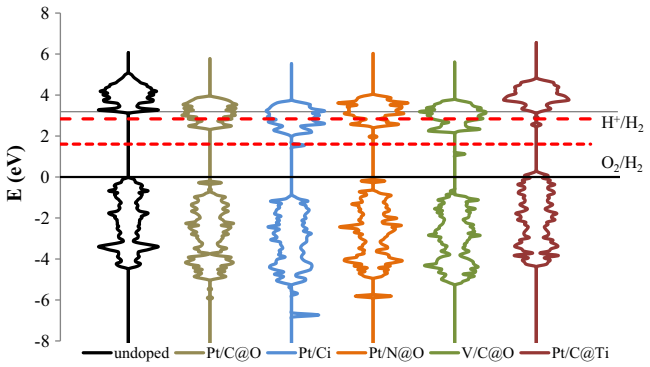

Fig. 5. Comparative density of states (DOS) of the different cases studied of co-doped anatase. The VBM of pure anatase is set to zero. A horizontal line is drawn on the conduction band bottom (CBM) of pure anatase as a guide for the eyes.

4. Conclusions

According to the first aim proposed, the results exhibit that the symmetrical structures found in the codoped systems are formed when the foreign nonmetal is located in anionic site, whatever the nature of the elements studied. On the other hand, we underline that the systems that have the highest interplanar spacing in the crystal structure are V-C@O and Pt-C@O, unlike Pt-N@O that has not shown significant modifications. In particular, the V-C@O would be applied as a good candidate to increase the surface area of the titania.

Finally, we point out that the most effective system to adjust the band gap alignment to enhance the redox reaction of H_2O to produce H_2 and O_2 is Pt-C@Ti because it presents the greatest narrowing of the band gap with respect to pure anatase, the lower shift of the conduction band and is the only one that favorably modifies the position of valence band, all are necessary conditions

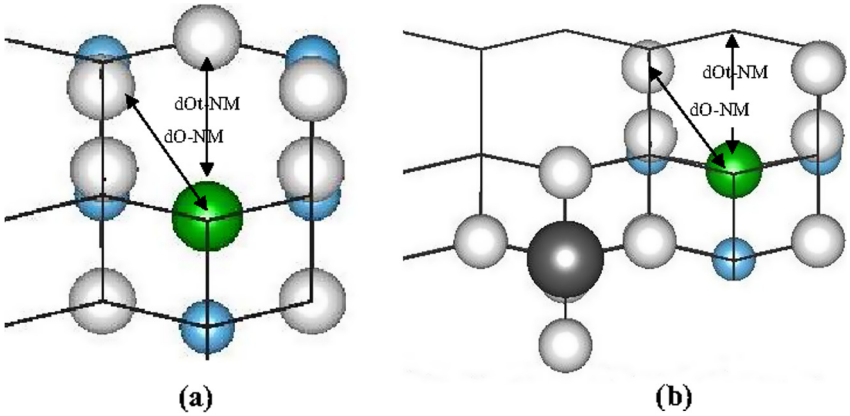

Fig. 6. Partial geometry of the monodoped (a) and codoped systems (b). The green/gray spheres represent NM (C or N)/M (Pt or V) impurities. Representative distances O-NM and Ot-NM which values are listed in Table 3 are also indicated. (For interpretation of the references to color in this figure legend, the reader is referred to the web version of this article.)

Table 3
The separation between the plane containing the NM impurity and the plane above it is represented by the distance between the NM and the O located just on top (Ot); see Fig. 6 for more details. The monodoped cases with carbon and nitrogen are included to facilite the comparison. Δd is the difference between dOt for codoped and the respective monodoped case.

	C@O	N@O	Pt-C@O	Pt-N@O	V-C@O
dO-NM	2.95	3.16	3.14	3.19	3.20
dOt-NM	3.47	3.83	3.75	3.86	3.86
Δd	–	–	0.28	0.03	0.39

for the mentioned reaction. For all other analyzed doped systems, the conduction bands are shifted to lower energies, unfavorable situation for the reduction reaction of H^+ and H_2 generation.

In summary, we have studied from first principles how different pairs of metal-nonmetal dopants affect the positions of the edge of the valence and conduction bands and consequently their redox potential in the search for the best candidate for water splitting into H_2 and O_2.

Acknowledgements

This work was in part supported by the Consejo Nacional de Investigaciones Científicas y Técnicas (CONICET) (PIP: 02286), Argentina and by the Universidad Nacional del Sur (UNS) (PGI: 24/F068), Argentina. The authors thank the use of computer facilities of GRUMASICA (GRUpo de MAteriales y SIstemas CAtalíticos).

References

[1] C.I.N. Morgade, G.F. Cabeza, Comput. Mater. Sci. 111 (2016) 513.
[2] Z. Zongyan, M. Zhaosheng, Zhigang, Chem. Phys. Chem. 13 (2012) 3836.
[3] A. Shokuhfar, M. Alzamani1, E. Eghdam, M. Karimi, S. Mastali, J. Nanosci. Nanotechnol. 2 (1) (2012) 16.
[4] Y. Hendrix, A. Lazaro, Q. Yu, J. Brouwers, World J. Nano Sci. Eng. 5 (2015) 161.
[5] A. Fujishima, K. Honda, Nature (London) 238 (1972) 37.
[6] A. Fujishima, K. Honda, Bull. Chem. Soc. Jpn. 44 (1971) 1148.
[7] S. Banerjee, J. Gopal, P. Muralledharan, A. Tyagiand, B. Raj, Curr. Sci. 90 (2006) 1378.
[8] L. Jinwen, R. Han, Y. Zhao, H. Wang, W. Liu, T. Yu, Y. Zhang, J. Phys. Chem. C 115 (2011) 4507.
[9] M. Grazel, Nature (London) 414 (2001) 338.
[10] J.M. Bolts, M.S. Wrighton, J. Phys. Chem. 80 (1976) 2841.
[11] Y. Matsumoto, J. Solid State Chem. 126 (1996) 227.
[12] H. Irie, Y. Watanabe, K. Hashimoto, Chem. Lett. 32 (2003) 772.
[13] X. Chen, C. Burda, J. Am. Chem. Soc. 130 (2008) 5018.
[14] T. Umebayashi, T. Yamaki, H. Itoh, K. Asai, J. Phys. Chem. Solids 63 (2002) 1909.
[15] J. Choi, H. Park, M.R. Hoffmann, J. Mater. Res. 25 (2010) 149.
[16] G. Kresse, J. Furthmuller, Phys. Rev. B 54 (1996) 11169.
[17] P. Blochl, Phys. Rev. B 50 (1994) 17953.
[18] J.P. Perdew, Y. Wang, Phys. Rev. B 33 (1986) 8800.
[19] M. Methfessel, A.T. Paxton, Phys. Rev. B 40 (1989) 3616.
[20] V. Anisimov, J. Zaanen, O. Andersen, Phys. Rev. B 44 (1991) 943.
[21] M. Cococcioni, S. de Gironcoli, Phys. Rev. B 71 (2005) 035105-1.
[22] S. Dudarev, G. Botton, S. Savrasov, C. Humphreys, A. Sutton, Phys. Rev. B 57 (1998) 1505.
[23] C.I.N. Morgade, Study of the properties of modified TiO_2 as a support for catalytic reactions (Ph.D. thesis), Universidad Nacional del Sur, Physics Department, 2015, December.
[24] C.I.N. Morgade, Ch.I. Vignatti, M.S. Avila, G.F. Cabeza, J. Mol. Catal. A: Chem. 407 (2015) 102.
[25] R.F.W. Bader, Atoms in Molecules: A Quantum Theory, Oxford University Press, Oxford, 1990.
[26] K. Momma, F. Izumi, J. Appl. Crystallogr. 44 (2011) 1272.
[27] H. Yan, X. Wang, M. Yao, X. Yao, Prog. Nat. Sci.: Mater. Int. 23 (2013) 402.
[28] O. Diwald, T. Thompson, E. Goralski, S. Walck, J. Yates, J. Phys. Chem. B 108 (2004) 52.
[29] D. Dolat, S. Mozia, B. Ohtani, A. Morawski, Chem. Eng. J. 225 (2013) 358.
[30] R. Dholam, N. Patel, A. Miotello, Int. J. Hydrogen Energy 36 (2011) 6519.
[31] X. Ma, L. Miao, S. Bie, J. Jang, Solid State Commun. 150 (2010) 689.
[32] J.C.-S. Wu, Ch-H. Chen, J. Photochem. Photobiol. A: Chem. 163 (2004) 509.
[33] K. Palanivelu, J. Im, Y. Lee, Carbon Sci. 3 (2007) 214.
[34] D. Feller, D.A. Dixon, J.S. Francisco, J. Phys. Chem. A 107 (2003) 1604.